Molecular Plant • Volume 2 • Number 2 • Pages 284–297 • March 2009 RESEARCH ARTICLE

Induction of the AOX1D Isoform of Alternative Oxidase in *A. thaliana* T-DNA Insertion Lines Lacking Isoform AOX1A Is Insufficient to Optimize Photosynthesis when Treated with Antimycin A

Inga Strodtkötter[a,2], Kollipara Padmasree[a,b,2], Challabathula Dinakar[a,b], Birgit Speth[a], Pamela S. Niazi[a], Joanna Wojtera[a], Ingo Voss[a], Phuc Thi Do[c], Adriano Nunes-Nesi[c], Alisdair R. Fernie[c], Vera Linke[a], Agepati S. Raghavendra[b] and **Renate Scheibe[a,1]**

a Department of Plant Physiology, FB5, University of Osnabrueck, 49069 Osnabrueck, Germany
b Department of Plant Sciences, School of Life Sciences, University of Hyderabad, Hyderabad 500 046, India
c Max Planck Institute for Molecular Plant Physiology, Am Mühlenberg 1, 14476 Potsdam-Golm, Germany

ABSTRACT Plant respiration is characterized by two pathways for electron transfer to O_2, namely the cytochrome pathway (CP) that is linked to ATP production, and the alternative pathway (AP), where electrons from ubiquinol are directly transferred to O_2 via an alternative oxidase (AOX) without concomitant ATP production. This latter pathway is well suited to dispose of excess electrons in the light, leading to optimized photosynthetic performance. We have characterized T-DNA-insertion mutant lines of *Arabidopsis thaliana* that do not express the major isoform, AOX1A. In standard growth conditions, these plants did not show any phenotype, but restriction of electron flow through CP by antimycin A, which induces AOX1A expression in the wild-type, led to an increased expression of AOX1D in leaves of the *aox1a*-knockout mutant. Despite the increased presence of the AOX1D isoform in the mutant, antimycin A caused inhibition of photosynthesis, increased ROS, and ultimately resulted in amplified membrane leakage and necrosis when compared to the wild-type, which was only marginally affected by the inhibitor. It thus appears that AOX1D was unable to fully compensate for the loss of AOX1A when electron flow via the CP is restricted. A combination of inhibition studies, coupled to metabolite profiling and targeted expression analysis of the P-protein of glycine decarboxylase complex (GDC), suggests that the *aox1a* mutants attempt to increase their capacity for photorespiration. However, given their deficiency, it is intriguing that increase in expression neither of AOX1D nor of GDC could fully compensate for the lack of AOX1A to optimize photosynthesis when treated with antimycin A. We suggest that the *aox1a* mutants can further be used to substantiate the current models concerning the influence of mitochondrial redox on photosynthetic performance and gene expression.

Key words: abiotic/environmental stress; acclimation—physiological; alternative electron transport; photorespiration; photosynthesis; mitochondria; T-DNA insertion line.

INTRODUCTION

Higher plant mitochondria possess two distinct pathways for the transfer of electrons from reduced ubiquinone to molecular oxygen: the cytochrome pathway (CP), which is sensitive to antimycin A (AA) and cyanide, and the alternative pathway (AP), which is insensitive to the aforementioned inhibitors, but is sensitive to salicylhydroxamate (SHAM) and propyl gallate. In the CP, electron transport is coupled to proton translocation and hence to ATP formation. Electron transport through the AP

[1] To whom correspondence should be addressed. E-mail scheibe@biologie.uni-osnabrueck.de, fax +49541/9692265, tel. +49541/9692284.

[2] Both authors contributed equally to this work.

doi: 10.1093/mp/ssn089, Advance Access publication 21 January 2009
Received 1 September 2008; accepted 13 November 2008

is, however, not linked to ATP production. The alternative oxidase (AOX), which mediates the terminal step of the AP, is localized to the inner membrane of mitochondria (Day and Wiskich, 1995; Siedow and Umbach, 2000; Finnegan et al., 2004). Initially, the identification of AP was identified as contributing to the '*thermogenesis*' associated with the attraction of insect pollinators (Meeuse, 1975). More recent studies indicate that both expression level and *in-vivo* engagement of the AOX are modulated by: (1) changes in cellular metabolism, (2) developmental stage, and (3) exposure to a range of biotic and abiotic factors (Juszczuk and Rychter, 2003; Millenaar and Lambers, 2003; Ho et al., 2007; Yoshida et al., 2007; Giraud et al., 2008). It is intriguing that AOX, whose function is not completely understood, is capable of responding to such a wide variety of signals (Clifton et al., 2006).

AOX is encoded by a small nuclear multigene family, which comprises at least two different subfamilies, AOX1 and AOX2. The number of genes coding for each subfamily of AOX varies among higher plants and also between monocots and dicots (Considine et al., 2002; Borecky et al., 2006). In *Arabidopsis*, five genes encoding the two subfamilies of AOX, namely AOX1A, AOX1B, AOX1C, AOX1D, and AOX2, have been identified, with each member subject to different cell-, tissue-, organ- or even stress-specific transcriptional regulation (Clifton et al., 2006). AOX1A is the major isoform in the leaf, and this isoform is induced by antimycin A, an inhibitor of the CP (Saisho et al., 2001). Microarray studies and quantitative RT–PCR analysis using *A. thaliana* have revealed up-regulation of *AOX1A* transcripts in many different types of stress treatments (Clifton et al., 2006). Moreover, the high sensitivity of AOX1A expression responses to antimycin A, organic acids, and ROS allows it to serve as a model for mitochondrial retrograde regulation of nuclear gene expression (Gray et al., 2004; Zarkovic et al., 2005). The role of AOX in alleviating ROS production is well documented in mitochondria as well as at the plant cellular and even tissue level, particularly in response to abiotic stresses such as low temperature (Maxwell et al., 1999; Fiorani et al., 2005; Umbach et al., 2005). Furthermore, the role of the AP in the protection of the photosynthetic electron transport chain (ETC) from the harmful effects of excess light was recently demonstrated in drought-stressed wheat (Bartoli et al., 2005; Pastore et al., 2007). Also, in a variegated mutant subjected to photooxidative stress, energy-dissipating systems of the mitochondria, including AOX1A expression, were induced (Yoshida et al., 2008).

AOX activity is additionally known to be modulated by several factors such as reduced ubiquinone, as well as changes in macronutrient availability (Vanlerberghe and McIntosh, 1997; Sieger et al., 2005). Apart from stress treatments, AOX protein abundance and *in-vivo* activity are also known to be regulated by the carbon and redox status of the cell (Vanlerberghe and Ordog, 2002). Indeed, the specific mitochondrial thioredoxin isoform (PtTrxh2) has the capacity to reduce AOX homodimers, enabling pyruvate activation (Gelhaye et al., 2004), and recent studies provide evidence for the physiological relevance of this activation process (Oliver et al., 2008).

There is increasing evidence for the importance of chloroplast–mitochondrial interactions in photosynthesis and respiration, at both biochemical and molecular levels (Hoefnagel et al., 1998; Atkin et al., 2000; Gardeström et al., 2002; Padmasree et al., 2002; Raghavendra and Padmasree, 2003; Matsuo and Obokata, 2006). While operation of the entire TCA cycle in the light is still under debate, several NAD(P)H dehydrogenases and uncoupling proteins linked to the mitochondrial electron transport chain have been demonstrated to be functional in the illuminated leaf (Graham, 1980; Krömer, 1995; Padmasree et al., 2002; Clifton et al., 2005; Tcherkez et al., 2005; Plaxton and Podestá, 2006; Sweetlove et al., 2006; Noctor et al., 2007; Nunes-Nesi et al., 2007a, 2007b; Rasmusson and Escobar, 2007; Noguchi and Yoshida, 2008; Nunes-Nesi et al., 2008; Yoshida et al., 2008). Interestingly, while deficiencies in the expression of genes related to certain enzymes of the TCA cycle, namely NAD–MDH and aconitase, enhanced plant photosynthetic performance and shoot growth of transgenic tomato leaves/plants (Carrari et al., 2003; Nunes-Nesi et al., 2005), restriction in mitochondrial electron transport or oxidative phosphorylation drastically decreased the photosynthetic performance of the mesophyll protoplasts from barley and pea (Krömer et al., 1993; Padmasree and Raghavendra, 1999a). Also, the CMSII mutants of *Nicotiana sylvestris* that lack a functional complex I of the mitochondrial ETC showed decreased photosynthetic capacity, prolonged induction periods and were unable to adjust to higher growth irradiances (Sabar et al., 2000; Dutilleul et al., 2003; Noctor et al., 2004; Priault et al., 2006). In addition, both the CP and the AP have been demonstrated, either by the use of chemical inhibition or by reverse genetic approaches, to help optimize photosynthesis in a number of ways, which include: (1) disposal of excess reducing equivalents from the chloroplast, exported through the malate valve (Krömer and Scheibe, 1996; Scheibe, 2004; Scheibe et al., 2005; Yoshida et al., 2007), (2) acceleration of photosynthetic induction and light activation of key chloroplastic enzymes (Padmasree and Raghavendra, 1999b, 2001) and (3) supply of ATP for cytosolic sucrose biosynthesis (Padmasree and Raghavendra, 1999c; Igamberdiev et al., 2006). Furthermore, the role of mitochondrial respiration in protecting photosynthesis against photoinhibition was demonstrated in mesophyll protoplasts of pea and in *Anacystis nidulans* and *Chlamydomonas reinhardtii* (Saradadevi and Raghavendra, 1992; Shyam et al., 1993; Singh et al., 1996).

In the present study, we employed both chemical and reverse genetic approaches in tandem, by analyzing *aox1a* mutants and simultaneously using the inhibitor antimycin A. Under standard conditions, no distinct mutant phenotype was detected, either at the whole plant level or in experiments conducted with leaf discs. However, application of the CP inhibitor, antimycin A, led to leaf tissue damage caused by inhibition of photosynthesis and a build-up of ROS in the *aox1a* mutants. These changes were paralleled by a clear induction of AOX1D and of the P-protein of the glycine decarboxylase complex (GDC). This finding led us to validate the results using

mesophyll protoplasts generated from wild-type and mutants following treatment with various inhibitors of the mitochondrial ETC and of photorespiration. Protoplasts offer the advantage that the cellular reactions are easily accessible to exogenously applied inhibitors and thus their effects can be recorded without delay. Results from these studies are discussed within the context of current models of the influence of mitochondria in photosynthetic processes.

RESULTS

Characterization of *aox1a*-Knockout Lines

We identified two independent *aox1a*–T-DNA knockout lines in *Arabidopsis*, named *At3g22370::*tDNA-133 and *At3g22370::*tDNA-53 that harbour a T-DNA insertion at positions 27914 and 28054, respectively, of chromosome 3 (see Supplemental Figure 1A). The combination of the *AOX1A* primers 53LP and 53RP for line 53 allowed amplification of a corresponding PCR product (958 bp) on genomic DNA from wild-type, but not from the homozygous *aox1a* line 53 (see Supplemental Figure 1B). For line 133, the gene-specific primers 133LP and 133RP were used, and the corresponding PCR product had a size of 996 bp (see Supplemental Figure 1C). PCR products could be amplified from genomic DNA of homozygous *aox1a* lines, but not wild-type, by combining T-DNA left border primers (LBa1 for line 53 and LB3 for line 133) and one gene-specific primer (see Supplemental Figure 1B and 1C). The amplified PCR product (950 bp for line 53 and 436 bp for line 133) was sequenced to determine the location of the T-DNA insertion within the *AOX1A* gene. PCR analysis of genomic DNA confirmed that the lines were homozygous.

Given that AOX1A is known to be expressed at low levels, and that its expression can be induced by treatment with antimycin A, we performed RT–PCR and Northern blot analyses in tissues after treatment with the inhibitor for 6 h or alternatively after high-light treatment. As shown in Supplemental Figure 1D–1F, the mutants lack the *AOX1A* transcript under all conditions. Moreover, Western blot analysis using the monoclonal antiserum against *Sauromatum guttatum* AOX (see Supplemental Figure 1G) (Elthon et al., 1989) revealed that both *aox1a* lines lack the AOX1A protein.

Phenotypic Appearance of *aox1a* Plants

Absence of AOX1A resulted in no alteration of phenotypic appearance under standard growth conditions (photoperiod of 7.5 h light, 16.5 h dark; Figure 1A). In contrast, when 5-week-old plants were treated with antimycin A, we observed profound differences between *aox1a* and wild-type plants (Figure 1B). In comparison to wild-type, the *aox1a* plants wilted and became necrotic when exposed to antimycin A. In contrast, the leaflets of wild-type plants were resistant, in spite of the disturbance in the electron flow through CP. The damaging effect of antimycin A on leaflets of *aox1a* mutants was clearly visible 6 d after the treatment under short-day photoperiod illumination at 50 $\mu E\ m^{-2}\ s^{-1}$ (Figure 1B).

Since an increase in intracellular ROS levels would be anticipated to damage the membranous structures of the cell, we next attempted to measure membrane leakage in the leaf discs exposed to antimycin A. In the presence of antimycin A, the leakage was very pronounced in leaf discs of *aox1a* plants (Figure 2). Wild-type discs treated with antimycin A as well as leaf discs of wild-type and *aox1a* plants that were not treated with antimycin A did not exhibit any sign of ion leakage. Given that the two insertion lines displayed exactly the same phenotypes, we focused further study exclusively on line 133.

Induction of *AOX1D* Transcripts in Leaf Discs of AOX1a-KO Plants upon Antimycin A Treatment

In order to test whether any of the other AOX isoforms were induced to compensate for the deficit of AOX1A in the knockout

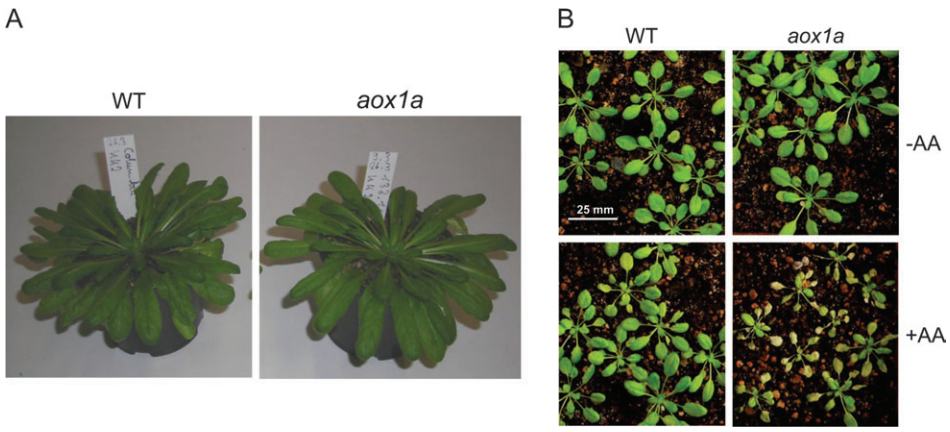

Figure 1. Growth Phenotype of *A. thaliana* Wild-type and *aox1a*-Knockout Plants.

(A) Phenotype of plants grown for 11 weeks under standard growth conditions. Plants were kept at 50 $\mu E\ m^{-2}\ s^{-1}$ under short-day photoperiod.

(B) Phenotypic appearance of the 5-week-old wild-type and *aox1a* plants growing under low light intensity (50 $\mu E\ m^{-2}\ s^{-1}$) and short-day photoperiod 6 d after treatment with 20 μM antimycin A (+AA) or water (−AA), respectively.

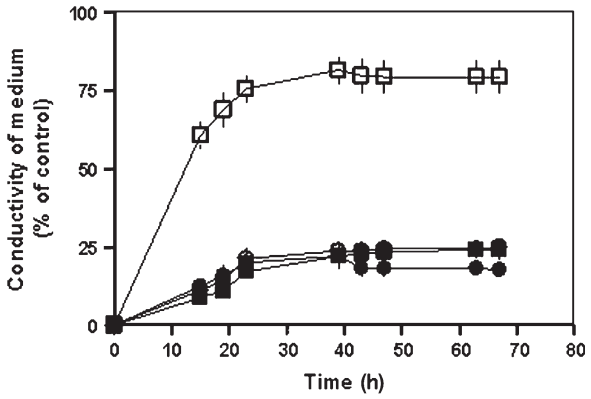

Figure 2. Ion Leakage from Leaf Discs of Wild-Type (Filled Symbols) and *aox1a* Plants (Open Symbols) after Pre-Incubating the Leaf Discs at 120 μE m^{-2} s^{-1} for 6 h in the Absence (●, ○) and Presence of 20 μM antimycin A (■, □).

Values are the mean of five independent measurements. The values of 100% conductivity were obtained by exposing the leaf discs to liquid N_2 prior to the transfer to water.

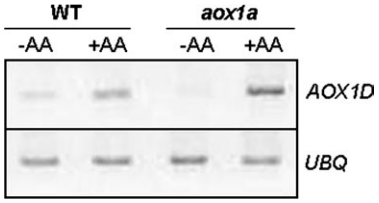

Figure 3. RT–PCR Analysis of *AOX1D* Expression in Wild-Type and *aox1a* Plants.

Total RNA was extracted from leaves discs either treated with (+AA) or without 20 μM antimycin A (–AA) in the light (120 μE m^{-2} s^{-1}) for 6 h. RT–PCR of AOX1D expression in wild-type and *aox1a* plants. PCR (25 cycles) was performed with *AOX1D*-specific primers.

plants, we subjected wild-type and mutants to Northern blot (see Supplemental Figure 2A) and RT–PCR analyses (Figure 3). Under standard conditions (6 h illumination at 120 μE m^{-2} s^{-1}), no *AOX1D* transcript was detected in leaf discs without antimycin A treatment. In contrast, after treatment with antimycin A, expression of AOX1D was enhanced in leaf discs of *aox1a* plants compared to wild-type. Expression levels of the other isoforms, namely AOX1B and AOX1C, in *aox1a* plants that were treated with antimycin A were unaltered (data not shown).

Antimycin A Causes Mutant-Specific Disruption of Photosynthetic Parameters

Since it is well known that mitochondria and chloroplasts are strongly interdependent in the light, a number of photosynthetic parameters were monitored in wild-type and *aox1a* plants, both under control conditions and following treatment with antimycin A (20 μM). Under control conditions, wild-type and *aox1a* lines display no significant differences in ΦII, qP, qNP, and F_V/F_M (Table 1). This indicates that photosynthetic electron flow is not affected in the knockout plants. Indeed, only following antimycin A treatment the photosynthetic electron transport was strongly affected in the *aox1a* plants in comparison to the wild-type. Under these conditions, a dramatic decrease in the F_V/F_M ratio indicates photoinhibition and possibly photodamage to PSII. In *aox1a* plants, the higher reduction state of Q_A of PSII in addition to the decreased quantum yield and an increase in qNP serve to support this hypothesis.

Metabolite Analyses of Wild-Type and *aox1a* Plants after Treatment with Antimycin A

Using GC–MS analyses for metabolites, we attempted to identify metabolic imbalances caused by the lack of AOX1A. Several differences between wild-type and *aox1a* mutants were detected under control conditions (full data set in Supplemental Table 1).

Table 1. Effect of Antimycin A Treatment on Various Photosynthetic Parameters in Wild-Type and *aox1a* Plants.

	Control		Treatment with antimycin A	
	Wild-type	*aox1a*	Wild-type	*aox1a*
F_V/F_M	0.72 ± 0.04	0.65 ± 0.1	0.65 ± 0.15	0.28 ± 0.12
qP	0.96 ± 0.03	0.92 ± 0.2	0.93 ± 0.01	0.79 ± 0.11
qNP	0.45 ± 0.08	0.33 ± 0.09	0.45 ± 0.17	1.87 ± 1.15
ΦII	0.67 ± 0.01	0.64 ± 0.04	0.63 ± 0.06	0.28 ± 0.12

Leaf discs from *A. thaliana* 12-week-old wild-type and *aox1a* plants were incubated without or with 20 μM antimycin A for 6 h under illumination. Prior to the measurements, the discs were kept in the dark for 1 h.

aox1a lines displayed significantly reduced levels of β-alanine and glutamate, while isoleucine levels increased. Interestingly, intermediates of the TCA cycle such as citrate and malate were significantly decreased in the mutant, while no changes were observed in succinate and fumarate levels. Under control conditions, the intermediates of the photorespiratory pathway: glycine, serine and glycerate—were not affected by the absence of AOX1A. When sugars were analyzed, trehalose and melezitose were significantly decreased in the mutant, while glucose, fructose, sucrose, raffinose, and ribose showed no changes.

Relative differences in metabolite profile became much more apparent after inhibition of CP with antimycin A. Indeed, we could observe significant differences from the wild-type for many metabolites (Supplemental Table 1). There was a significant relative increase in the amino acids γ-amino butyric acid (GABA), glycine, methionine, while the serine value showed a relative decrease. However, no significant changes in proline, alanine, phenylalanine, and valine levels were observed. Pyruvate increased more than four-fold in the knockout plants compared to the wild-type upon antimycin A treatment, while citrate decreased (Figure 4). When we analyzed the TCA-cycle intermediate levels, similar results to untreated samples were observed in the antimycin A-treated samples, except for a relative increase in 2-oxoglutarate. It was apparent that there was a significant reduction of malate and citrate levels, while 2-oxoglutarate increased (Figure 4). Interestingly, there was also a six-fold increase in 4-hydroxybutyrate, a by-product of GABA

catabolism, in the *aox1a* mutant after inhibition of CP with antimycin A (Figure 4). As in untreated samples, sugars such as glucose, fructose, galactose, and raffinose did not change in treated samples, while only maltose increased (Supplemental Table 1).

Effects on Photorespiration

From the metabolite analysis (Figure 4), it became apparent that relative glycine and serine levels showed opposite trends. To gain absolute quantification of this, we performed calibration curves with authentic standards of these amino acids (Figure 5A). When leaf discs of wild-type and *aox1a* plants were incubated with 20 μM antimycin A in the light for 6 h, the glycine-to-serine ratio increased to 4.6 as compared to 0.6 in wild-type (Figure 5B). According to the cross-over theory (Rolleston, 1972), these changes are indicative of a limitation at the GDC-catalyzed step. We used specific probes as well as antibodies against the P-protein of GDC to see whether differences at the metabolite level could be traced to changes in the enzyme complex. While the transcript level for P-protein was increased in the mutant compared to wild-type, both in controls and

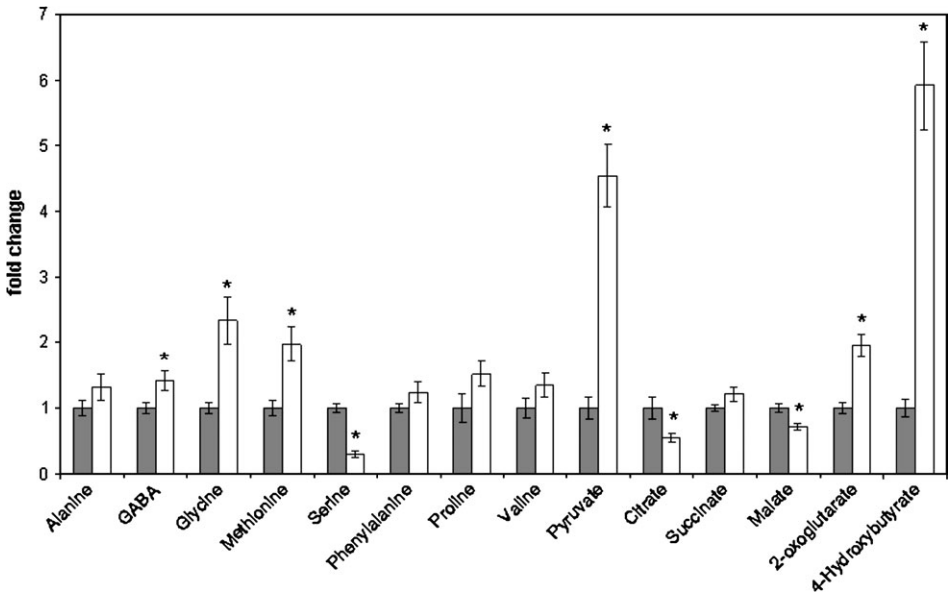

Figure 4. Relative Metabolite Content in Leaf Discs of Wild-Type (Grey Bars) and *aox1a* Mutants (White Bars) Plants after Antimycin A Treatment (20 μM).

Data are normalized with respect to the mean response calculated for the wild-type. Values are presented as mean ± S.E. of determinations on six replications per genotype. An asterisk indicates values that were determined by the *t*-test to be significantly different ($P < 0.05$) from the wild-type.

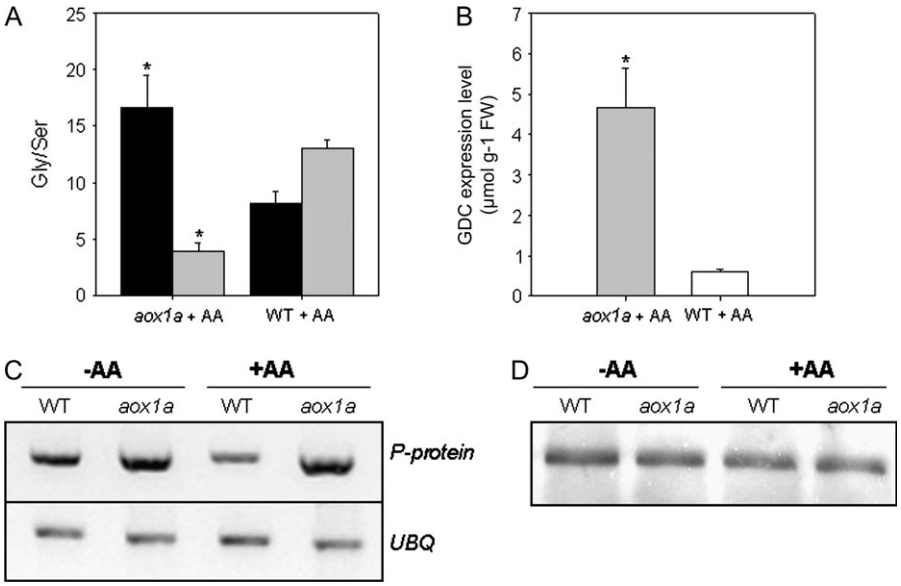

Figure 5. (A) Glycine and Serine Content and Expression level of Glycine Decarboxylase. Absolute Values for Glycine (Black Bars) and Serine (Grey Bars).

(B) Glycine-to-serine ratio of *aox1a* discs (gray bar) and wild-type (white bar) after antimycin A treatment (20 μM).

Values in A and B are presented as mean ± S.E. of six individual determinations per genotype. An asterisk indicates values that were determined by the *t*-test to be significantly different ($P < 0.05$) from the wild-type.

(C) RT–PCR analysis of GDC (P-protein) expression in leaf discs of wild-type and *aox1a* plants incubated in H_2O with and without addition of 20 μM antimycin A.

(D) Western blot and immunodetection using antiserum against the P-protein of GDC were performed with extracts from wild-type and *aox1a* plants after antimycin A treatment .

following antimycin A treatment (Figure 5C), the Western blot result suggests that there are at least equal amounts of P-protein in wild-type and mutant under both conditions (Figure 5D). Therefore, a limitation at this step cannot be due to lack of the GDC protein; however, the protein might be non-functional or at least display reduced functionality in the mutant.

Photosynthetic Performance and Respiratory Rates of Protoplasts from Wild-Type and *aox1a* Plants

Photosynthetic and respiratory performance of mesophyll protoplasts isolated from *aox1a* plants was examined using an oxygen-electrode chamber. At saturating light intensities and bicarbonate levels, the rates of O_2 evolution exhibited by protoplasts prepared from the *aox1a* mutants (137 $\pm$ 15 μmoles mg^{-1} Chl h^{-1}) were comparable to the rates of mesophyll protoplasts prepared from wild-type plants (124 $\pm$ 10 μmoles mg^{-1} Chl h^{-1}) (Figure 6A). While there was a moderate inhibition (<30%) of photosynthesis by antimycin A (20 μM) in wild-type protoplasts, SHAM (10 mM) drastically reduced photosynthesis to 10% of the control rate. By contrast, in the *aox1a* protoplasts, both inhibitors decreased the rate of photosynthesis to 45–50% of the control rates (Figure 6A).

In comparison to wild-type mesophyll protoplasts, those isolated from *aox1a* plants had similar rates of total respiratory O_2 consumption under standard conditions (16.5 $\pm$ 1.0 and 16.0 $\pm$ 0.8 μmoles mg^{-1} Chl h^{-1}, respectively), but differed from wild-type in the presence of antimycin A (20 μM), and of SHAM (10 mM) (Figure 6B). In the presence of antimycin A, the decrease in O_2-consumption rate was higher in *aox1a* (69%) than in wild-type (55%). By contrast, in the presence of SHAM, the decrease in the rate of O_2 consumption was greater in protoplasts from wild-type plants (45%), when compared to protoplasts from *aox1a* plants (38%) (Figure 6B). Most interestingly, the *aox1a* plants could be still inhibited by SHAM. This result is in accordance with the induction of another AOX isoform in the mutants (as demonstrated in Figure 3).

Effect of Inhibition of Photorespiration on Photosynthesis in Isolated Protoplasts

We examined the photosynthetic performance of isolated protoplasts from *aox1a* mutants in more detail. Since photorespiration could serve as an alternative dissipating system, photosynthesis was monitored in the absence and in the presence of aminoacetonitrile (AAN, inhibitor of glycine decarboxylase). Most striking was the fact that AAN, up to concentrations of 10 mM, only marginally affected photosynthesis in *aox1a* protoplasts, while decreasing photosynthesis by <60% in wild-type (Figure 7).

Effect of Antimycin A on the Adenylate Status in Protoplasts from *aox1a* and Wild-Type Plants

Isolated intact protoplasts were illuminated in the presence and absence of antimycin A and subjected to ATP/ADP analysis. There was no major effect of antimycin A on the ATP/ADP ratio in wild-type, while the high ATP/ADP ratio in the *aox1a* protoplasts was brought down by antimycin A (Figure 8).

Effect of Antimycin A on Intracellular ROS Production

Intracellular ROS generation was measured as DCF fluorescence using mesophyll protoplasts after exposure to antimycin A, during induction (Figure 9A) and steady-state photosynthesis (Figure 9B), respectively. When mesophyll protoplasts from *aox1a* mutants were treated with antimycin A in the light, the rise in DCF fluorescence was significant during both the induction period (from 1.8- to 3.2-fold) and steady-state photosynthesis (from 2.7- to 9.2-fold). By contrast, in wild-type protoplasts, the increase of DCF fluorescence on treatment with antimycin A was relatively small. Our results were in agreement with those obtained with *A. thaliana* antisense lines that showed marked increase of oxidative damage in leaf tissues incubated with SHAM and KCN together when compared to leaf tissues incubated with KCN alone (Umbach et al., 2005).

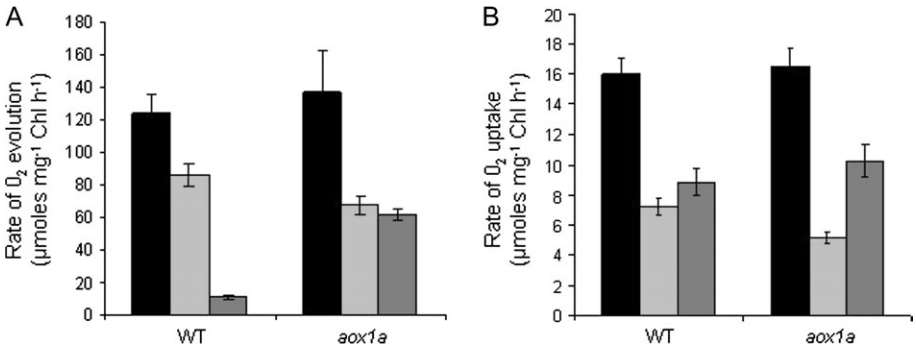

Figure 6. Photosynthetic O_2 Evolution **(A)** and Respiratory O_2 Uptake **(B)** of Mesophyll Protoplasts from Wild-Type and *aox1a* Plants.
Photosynthesis and respiration were measured without addition of an inhibitor (black bars), with addition of 20 μM antimycin A (light-grey bars), and with addition of 10 mM SHAM (dark-grey bars). The O_2-evolution rates were examined after 10 min of illumination during steady-state photosynthesis. Respiratory O_2 uptake rates were taken after 5 min of dark period.

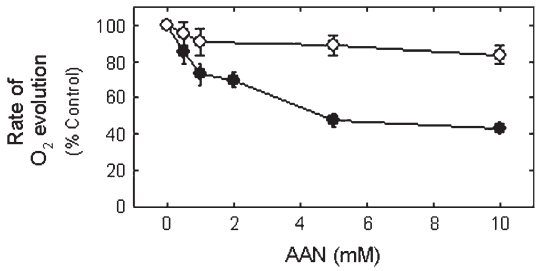

Figure 7. Photosynthetic O_2 Evolution of Mesophyll Protoplasts from Wild-Type (Closed Circles) and *aox1a* Plants (Open Circles).
The rate of O_2 evolution was measured at a light intensity of 1000 μE m^{-2} s^{-1} and in the presence of 1 mM bicarbonate. In addition, AAN was present at the indicated concentrations. One hundred % activity corresponds to 125.3 μmoles mg^{-1} Chl h^{-1} for wild-type and 136.6 μmoles mg^{-1} Chl h^{-1} for *aox1a* plants, respectively.

We corroborated the increased level of ROS in *aox1a* protoplasts upon antimycin A treatment using laser scanning fluorescence microscopy, after adding the membrane-permeant dye CM-H_2DCF-DA, which becomes fluorescent upon oxidation by ROS (Figure 9C and 9D). In the *aox1a* mutant, more protoplasts displayed fluorescence than in the wild-type, especially after treatment with antimycin A.

DISCUSSION

Any imbalance between the generation and utilization of energy equivalents leads to over-energization of thylakoid membranes, ultimately resulting in inhibition of photosynthesis. Higher plants have evolved several mechanisms to prevent such over-reduction of the chloroplastic thylakoid membrane components. These mechanisms involve either chloroplasts (Scheibe et al., 2005), or mitochondria (Raghavendra and Padmasree, 2003; Yoshida et al., 2006, 2007). AOX is an important mitochondrial enzyme associated with at least three major functions in plant tissues: (1) to keep the TCA cycle active, even under conditions when the cellular demand for ATP is very low (Vanlerberghe and Ordog, 2002), (2) to avoid ROS formation when electron transport through the CP is restricted (Maxwell et al., 1999; Umbach et al., 2005; Amirsadeghi et al., 2006), and (3) to dissipate excess reducing equivalents generated in chloroplasts during illumination (Padmasree and Raghavendra, 1999c; Yoshida et al., 2007, 2008).

Phenotype in *aox1a* Plants Is Only Evident upon Inhibition with Antimycin A

As the mutants lacking AOX1A resembled wild-type morphologically in their phenotype (Figure 1), energy normally dissipated through AP must have been diverted to other metabolic pathways. It is somewhat surprising that plants lacking AOX1A only revealed oxidative damage when CP was blocked by antimycin A. However, this may be due to the fact that the plants in the present work were grown at very moderate light intensities, and that the role of AOX only becomes evident when CP was additionally restricted.

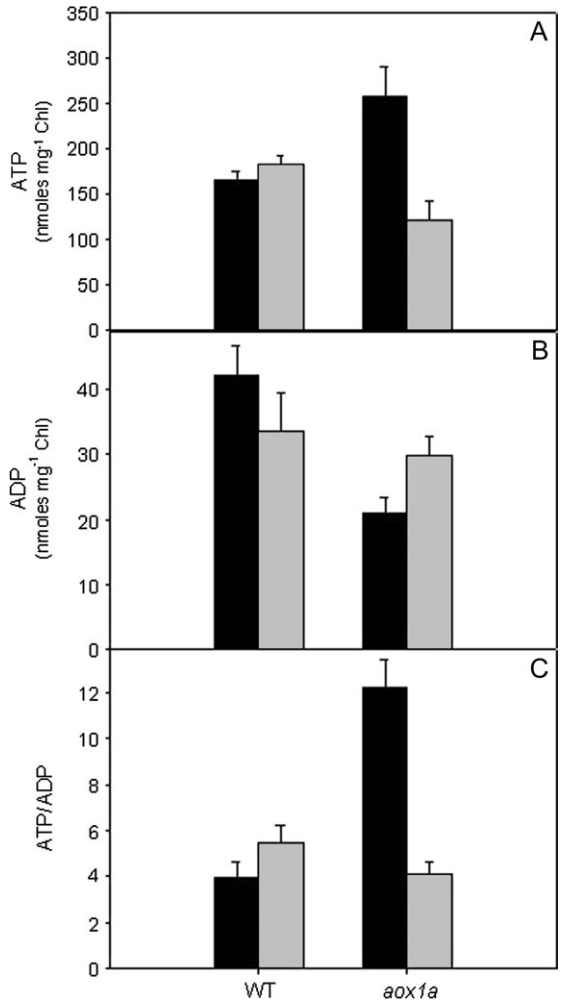

Figure 8. Total Content of ATP **(A)**, ADP **(B)**, and Corresponding ATP/ADP Ratios **(C)**, Respectively, in Protoplasts of Wild-Type and *aox1a* Plants as Affected by Antimycin A Treatment in the Light.
ATP and ADP were determined in protoplasts exposed for 10 min to light in the absence (black bars) or presence of 0.1 μM antimycin A (gray bars).

There have been several studies wherein the importance of AP was contrasted with CP and/or antioxidants and ROS-scavenging systems (Dutilleul et al., 2003; Bartoli et al., 2005; Sieger et al., 2005). The present publication emphasizes the important role of AOX1A in sustaining carbon assimilation, optimizing carbon flux through photorespiration and preventing ROS formation, particularly when electron transport through the CP is restricted by incubation with antimycin A. The experiments using leaf discs demonstrated the effect after induction of AOX1D expression in *aox1a* plants on treatment with antimycin A. In a complementary approach, the experiments on mesophyll protoplasts revealed the short-term effects of restricting mitochondrial oxidative metabolism by antimycin A on photosynthetic and respiratory rates and on ROS formation when AOX1A was lacking.

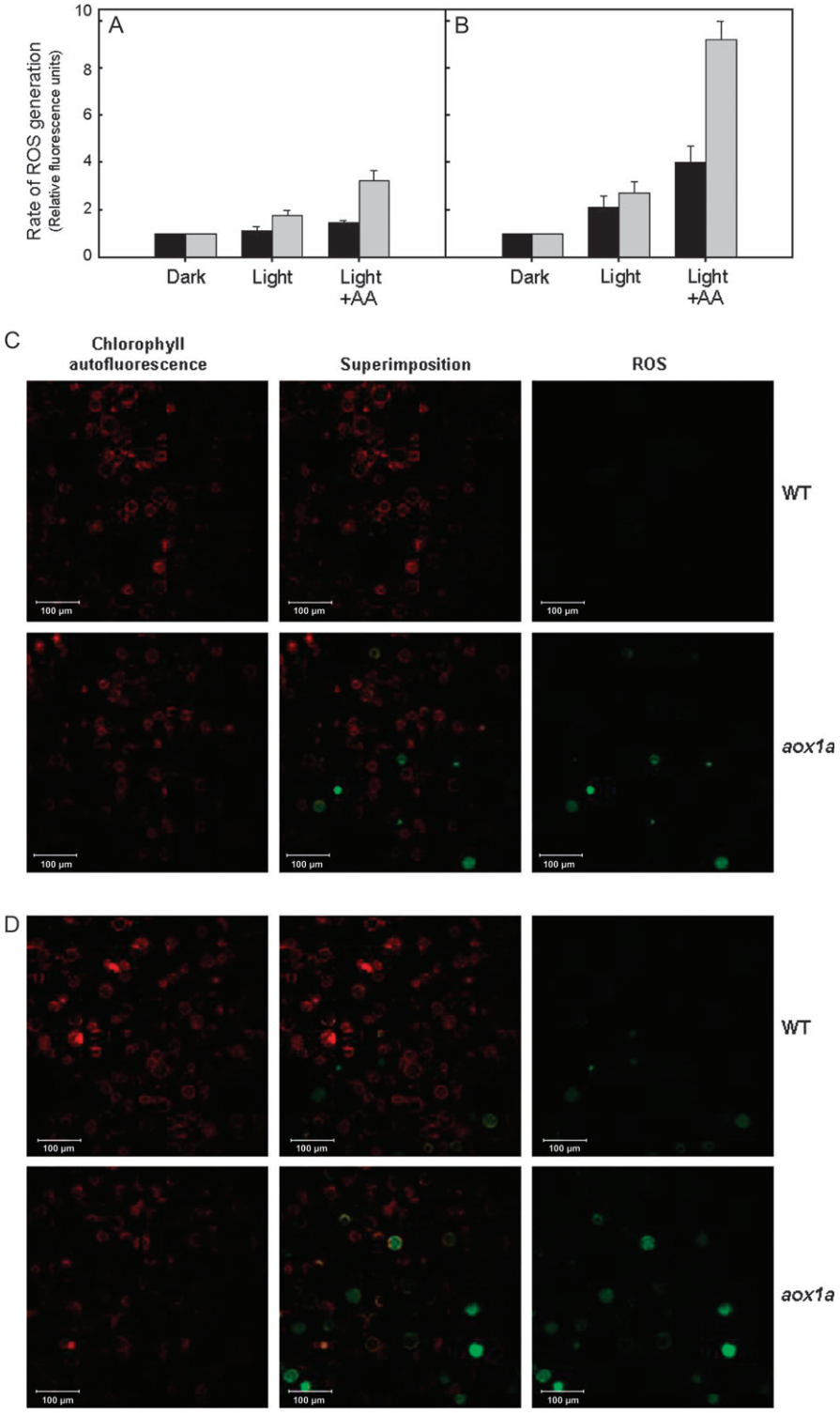

Figure 9. Measurement of ROS Formation during Photosynthetic Induction after 2 min **(A)** and During Steady-State Photosynthesis after 10 min **(B)** in Mesophyll Protoplasts from Wild-Type (Black Bars) and *aox1a* Plants (Grey Bars), Respectively.

The mesophyll protoplasts were exposed to 1000 µE m^{-2} s^{-1} either in the absence (control samples) or presence of 0.1 µM antimycin A (treated samples). DCF fluorescence was determined after 2 or 10 min, respectively. In addition, protoplasts were stained with 0.1 µM CM-H_2DCF-DA after an illumination period of 6 h at 120 µE m^{-2} s^{-1}, in the absence **(C)** or presence **(D)** of 0.1 µM antimycin A. Protoplasts were observed by confocal laser scanning microscopy. Chlorophyll autofluorescence is shown in red, ROS (stained by CM-H_2DCF-DA) is shown in green. An overlay of both images is displayed.

We hypothesize that there are two possibilities for the adaptation and the normal phenotypic appearance of *aox1a* plants (Figure 1). While the first possibility is an adjustment in the transcript level of different AOX isoforms, the second possibility would be due to metabolic adjustments. The results obtained in our present study indicate that both mechanisms contribute to the adjustment of the *aox1a* mutant, as indicated by (1) increase of another isoform, namely AOX1D (Figure 3); (2) decrease in the sensitivity of photosynthetic O_2 evolution to the photorespiratory inhibitor AAN (Figure 7); and (3) use of alternative pathways for consumption of excess reducing equivalents (Figure 5).

Metabolic and Transcriptional Flexibility of *aox1a* Mutants Prevents Damage

The respiratory oxygen uptake rates of aox1a mutants were similar to wild-type plants (Figure 6B). This was possibly due to the increased rates of electron transport through CP, as indicated by the stronger suppression of respiratory O_2 uptake in the presence of antimycin A by mesophyll protoplasts than of that in wild-type plants (Figure 6B), and the increased expression of other isoforms of AOX, namely AOX1D, in aox1a plants (Figure 3). The sharp decline in the rate of respiratory O_2 uptake in presence of SHAM also demonstrated the continued participation of AP in maintaining normal respiratory O_2 consumption rates in aox1a plants (Figure 6B). While, in most studies with leaves, the isoform AOX1A was found to respond to stress, an increase in isoform AOX1D was detected in mutant plants that lack a functional complex III of the ETC (Zsigmond et al., 2008). Such coordination of different AOX isoform expression is not surprising, in view of the flexibility exhibited by AOX in CMSII mutants, which are impaired in mitochondrial complex I, a major sink for NADH (Gutierres et al., 1997; Sabar et al., 2000).

The persistent sensitivity of photosynthetic O_2 evolution to the AP inhibitor SHAM indicated genetic and biochemical adjustments in *aox1a* mutants. This hypothesis was further corroborated by increased AOX1D expression in these mutants when they were treated with antimycin A. The changes observed in the mutant (Figure 4) suggest the modulation of mitochondrial metabolites, particularly 4-hydoxybutyrate, 2-oxoglutrate, citrate, malate, GABA, and methionine. However, a detailed and direct evaluation of the role these metabolites play in the readjustment of the mutant remains to be attempted. It is possible that enhanced pyruvate levels in the *aox1a* mutants activate the up-regulated AOX isoform (AOX1D) by modulating its redox-sensitive regulatory sulfhydryl/disulfide group as has been recently documented for transgenic potato lines down-regulated in the expression of pyruvate kinase (Oliver et al., 2008). The increase in glycolytic intermediates such as 2-oxoglutarate and metabolites associated with the GABA shunt most likely reflect a back-up of the classical pathways that supply the mitochondrial transport chain (Plaxton and Podestá, 2006).

The transcript levels of *AOX1D* were up-regulated (Figure 3), along with the increases in total cellular ROS levels (Figures 9) when electron transport through the CP was restricted with antimycin A. The differential response of *AOX1D* is in accordance with the experiments of Gray et al. (2004) and Zarkovic et al. (2005), which suggested induction of AOX expression by distinct, ROS-specific and organic acid-specific signaling pathways from mitochondria to the nucleus. This situation raises intriguing questions, such as whether *AOX1D* is subject to redox or metabolic regulation at the translational and post-translational levels. Furthermore, recent reports have associated *AOX1D*-transcript level abundance with senescence and adjustments to nitrogen supply in leaf tissues and to abiotic stress (Clifton et al., 2006; Escobar et al., 2006; Zsigmond et al., 2008). So far, to our knowledge, alterations in the expression of AOX1D have not been reported at the protein level.

Photorespiration Is a Possible Alternative Electron Sink

The carbon flux through GDC appears to have been affected, as indicated by the increase in glycine, along with the decrease in serine, in the mutants. Such a situation may result when the protein levels and/or the activity of GDC are lowered. We could detect an increased transcript level of the P-protein of GDC and an unchanged protein level for this GDC subunit in *aox1a* plants, irrespective of the presence of antimycin A (Figure 5C and 5D). Although we did not check the actual activity of GDC, our aim here was merely to indicate that photorespiratory metabolism is strongly modulated when AOX1A is lacking.

We also observed an increase in the ATP level as well as in the ATP/ADP ratio in *aox1a* plants (Figure 8). This is most probably indicative of an increased flux through CP in order to cope with the reducing equivalents. On antimycin A treatment of the knockout plants, NADH from glycine decarboxylation cannot be re-oxidized, neither by AP, nor by CP. Therefore, NADH builds up, which might eventually lead to feedback inhibition of GDC and an increased Gly/Ser ratio (Figure 5B). Alternatively, the expressed protein might be non-functional.

It appears that the plant attempts to counter these effects by elevating the levels of GDC and AOX1D expression, but that this in itself cannot overcome the inhibition caused by antimycin A. When taken together, the results of the current study suggest that AOX, particularly the AOX1A isoform, plays a significant role in dissipating chloroplastic reducing equivalents, in coordination with CP, to optimize photosynthetic performance.

Concluding Remarks

In conclusion, we show that plants try to compensate for the lack of AOX1A by using alternative mechanisms. Upon restriction of the CP by antimycin A, the isoform AOX1D was induced and GDC levels were increased, but these could not protect photosynthesis in *aox1a* plants against the inhibition caused by antimycin A. We suggest that AOX, particularly the AOX1A isoform, plays a significant role in dissipating chloroplastic reducing equivalents in coordination with CP to optimize photosynthetic performance.

METHODS

Cultivation of Plant Material

Wild-type and transgenic *Arabidopsis thaliana* (ecotype Columbia) were cultivated in a growth chamber in soil at 20°C with a light intensity of 50 $\mu E\ m^{-2}\ s^{-1}$. Light was present for 7.5 h per day. For stress conditions, plants were exposed to antimycin A and/or high light (800 $\mu E\ m^{-2}\ s^{-1}$) for the indicated times.

aox1a Mutant Screen

Seeds of the *Arabidopsis aox1a* mutant lines *At3g22370::* tDNA-53 (Salk_084897) and *At3g22370*::tDNA-133 (Sail_303_D04) were obtained from the Arabidopsis Biological Resource Centre (www.arabidopsis.org/abrc). Homozygous knockout plants were identified by PCR to detect a T-DNA insertion within the gene region of *At3g22370*. Genomic DNA was isolated from plant tissues by standard methods. The sequence information for the gene- and T-DNA-specific primers was taken from the SALK-Institute (http://signal.salk.edu). The insertion position of the T-DNA products was checked by sequencing the PCR products.

Extraction of Total RNA and Northern Blot Analysis

For Northern blot analysis, total RNA was isolated from frozen leaf material using the Purescript RNA extraction kit (Gentra Systems, Minneapolis, MN, USA). For RNA gel-blot hybridization analysis, 10 μg of total RNA were denatured and separated on a 1.0% (w/v) agarose 2.5% (v/v) formaldehyde gel. Homidium bromide was included in the loading buffer to quantify equal sample loading. RNA was blotted onto a nylon membrane (Hybond-N, Amersham Biosciences) by downstream capillary transfer. RNA was cross-linked to the membrane by UV irradiation. Prehybridization and hybridization were performed at 65°C in Church buffer medium (0.25 M sodium phosphate, pH 7.2, 1 mM EDTA, 7% (w/v) SDS, and 1% bovine serum albumin (BSA)). Hybridization was performed with an α-[^{32}P]-dCTP-labeled *AOX1A*(*A.t.*) cDNA-specific probe (Ready-To-Go DNA labeling beads, Amersham Biosciences). Membranes were washed twice for 15 min at 65°C in washing buffer (40 mM sodium phosphate, pH 7.2, 1 mM EDTA, 0.5% (w/v) SDS and 0.5% (w/v) BSA, then for 10 min at room temperature in washing buffer containing 1% (w/v) SDS. Finally, membranes were exposed to a Phospho-Imager (GE Healthcare, Freiburg).

RT–PCR

Non-competitive RT–PCR was performed essentially as described by Ahn (2002). The cDNA was synthesized from 5 μg total RNA using oligo(dT) as primers according to the manufacturer's instructions (Fermentas RevertAid™ First Strand cDNA Synthesis Kit, Fermentas GmbH, St Leon-Rot, Germany). For a 25-μl PCR reaction, 1 μl of cDNA was used as template. The PCR settings were: first cycle at 95°C for 5 min, then for the optimized number of cycles of each gene product 1 min at 95°C, 1 min at 47–67°C and 1 min at 72°C and a final extension at 72°C for 5 min. For the detection of the transcripts, we used the following oligonucleotides: At3g22370 (*AOX1A*) (5′-CGTGTGAAGCGTATAAAGACGACAA-3′) and (5′-CCAAGTATGGCTTAAGCAGAGGTGA-3′); At1g32350 (*AOX1D*) (5′-CCCCAACTGTTGTTACTCATG-3′) and (5′-CTTTA-ATGATATCCAATAGGAGCC-3′) and At4g33010 (p-protein 1): (5′-TACTTACATTGCCATGATGGGATCTG-3′) and 5′-GCAGCTGC-GACTTGTTCTTCCTCT-3′).

Western Blot and Immunodetection

Equal amounts of soluble protein (25 μg) were loaded on two 10% discontinuous SDS–polyacrylamide gels using a vertical minigel system. The gel was blotted onto PVDF membrane. Immunodetection was performed essentially as described in Graeve et al. (1994). For the detection of AOX1A, the monoclonal antiserum against AOX (Elthon et al., 1989) (1:100) was used. For the detection the secondary antibody anti-mouse-IgG coupled to alkaline phosphatase (1:2000) and nitro blue tetrazolium and 5-bromo-4-chloro-3-indolyl phosphate as substrates were utilized. The protein contents of leaf extracts were determined according to Bradford (1976), with bovine serum albumin as a standard.

Antimycin A Treatment

The 5-week-old plants were sprayed with 20 μM antimycin A prepared in 0.01% Tween-20, and the controls were treated with 0.01% Tween-20 in water alone. Leaf discs were placed in a Petri dish upside down on the surface of water with, and in the case of the controls without, addition of 20 μM antimycin A. The leaf discs were illuminated from below. For the experiments with the mesophyll protoplasts, the incubation medium contained 0.1 μM antimycin A (treated samples), or antimycin A was omitted (control samples).

Chlorophyll Fluorescence and P700 Measurement in Leaf Discs

Delayed chlorophyll fluorescence was determined by the saturation-pulse method according to Schreiber et al. (1986) using a PAM-101 fluorimeter with integrated PAM-103 (Walz, Effeltrich, Germany). Actinic light (120 μE m^{-2} s^{-1}) was applied using a KL1500 with a white-light halogen lamp (Schott, Hohenheim, Germany), and the saturating light pulses (SP) (3000 μE m^{-2} s^{-1} for 800 ms) were generated by the FL-103 (Walz, Effeltrich, Germany) equipped with a 300-W cold-light source.

Calculated quantum yield of PS II (ΦII) and of the quenching coefficients qP and qNP were calculated according to Schreiber et al. (1986) and Genty et al. (1989) using the following equations: $\Phi II = [F_{V(S)} - F_V]/[F_0 - F_{V(S)}]$; $qP = [F_{V(S)} - F_V]/F_{V(S)}$; $qNP = [F_M - F_{V(S)}]/F_{V(S)}$ and $F_V/F_M = [F_M - F_0]/F_M$.

The measurements were carried out with leaf discs (1.54 cm^2) from wild-type and *aox1a* plants pre-incubated for 6 h in the presence and absence of 20 μM antimycin A at 120 μE m^{-2} s^{-1}, followed by a 30-min dark period before chlorophyll-fluorescence quenching and P700-redox state measurements were performed at the defined light intensities. For each measurement, two leaf discs were used from each of three independent plants, and the experiment was repeated two to four times.

Conductivity Measurement

The permeability changes in the leaf discs on exposure to antimycin A were detected using a conductivity meter with one

disc in a volume of 5 ml double-distilled water. The 100% value was obtained after freezing in liquid N_2 and subsequent thawing of the leaf material in the water.

Isolation of Mesophyll Protoplasts

Mesophyll–cell protoplasts were isolated from leaves of wild-type and *aox1a* plants of between 11 and 12 weeks of age, maintained under the growth conditions as described above. The peeled leaf pieces without midrib were subjected to enzymatic digestion with 1% (w:v) Cellulase Onozuka R-10 and 0.4% (w:v) Macerozyme R-10 as described in detail elsewhere (Riazunnisa et al., 2007).

Monitoring Photosynthetic and Respiratory Performance

Respiratory O_2 uptake in the dark and photosynthetic O_2 evolution in the light by mesophyll protoplasts of wild-type and knockout plants were monitored at 25°C using a Clark-type O_2 electrode (Model DW2, Hansatech Ltd, King's Lynn, UK). The reaction medium for both photosynthesis and respiration was 1 ml containing 0.65 M sorbitol, 1 mM $CaCl_2$, 1 mM $MgCl_2$, and 1 mM $NaHCO_3$ in 10 mM Hepes-KOH, pH 7.5, and protoplasts equivalent to 10 μg Chl (Riazunnisa et al., 2007). Illumination of 1000 μE m^{-2} s^{-1} was provided by a 35-mm slide projector (halogen lamp: Xenophot 24V:150W). The inhibitors antimycin A, SHAM, and AAN were added to the reaction medium containing mesophyll protoplasts to obtain the required final concentration, and the protoplasts were pre-incubated in darkness at 25°C for 5 min before switching on the light.

Detection of ROS Using Spectrofluorometry

The intracellular levels of ROS in mesophyll protoplasts were determined using 2′,7′-dichlorofluorescein diacetate (H_2DCF-DA, Molecular Probes) by modifying the protocol described in Maxwell et al. (1999). Mesophyll protoplasts were pre-incubated for 30 min with H_2DCF-DA (100 μM). Subsequently, the mesophyll protoplasts were subjected to centrifugation twice for 5 min at 1000 rpm, so as to dilute the final concentration of H_2DCF-DA to 5 μM. Fluorescence was measured using the SLM-AMINCO spectrofluorometer (Model 8100) with excitation and emission wavelengths set at 488 and 525 nm, respectively.

Detection of ROS Using Confocal Laser-Scanning Microscopy

To quantify ROS development, isolated treated protoplasts were stained with 0.1 μM 5-(and 6)-chloromethyl-2′,7′-dichlorodihydrofluorescein diacetate, acetyl ester (CM-H_2DCF-DA) as described in Voss et al. (2008). The images in Figure 9C and 9D were taken from a confocal laser-scanning microscope system (LSM 510 META; Zeiss, Göttingen, Germany) with a 20× EC Plan Neofluor (N.A. 1.3) oil objective. CM-H_2DCF-DA signals and autofluorescence of chlorophyll were visualized with excitation at 488 nm and emission at 500–530 and 650–710 nm, respectively. All images were scanned using the same parameters, such as laser power, detector gain, offset, pinhole, and zoom, in order to maintain comparable imaging conditions.

Metabolite Profiling

Metabolite analysis was performed by gas chromatography–mass spectrometry (GC–MS) as described by Lisec et al. (2006), with the exception that the absolute levels of glycine and serine were quantified as detailed in Roessner-Tunali et al. (2003).

Adenylate Quantitation

ATP and ADP were estimated according to Padmasree and Raghavendra (1999a). Aliquots of protoplast samples containing 100 μg Chl were withdrawn from the oxygen electrode chamber after 10 min of illumination and added to 70% $HClO_4$, to make a final concentration of 3% (v:v). The mixtures were frozen in liquid nitrogen until used. The samples were then thawed and centrifuged at 7000 *g* for 10 min. The supernatant was neutralized with KOH triethanolamine and left on ice for 30 min. The neutralized samples were centrifuged at 7000 *g* and the cleared supernatant was used for estimation of ATP and ADP. The levels of ATP were measured using enzymatic assays coupled to NADPH formation, while ADP levels were measured by coupling to NADH utilization.

The reaction medium for the assay of ATP (1 ml) contained 150 mM triethanolamine buffer, pH 7.5, 0.5 mM NADP, 10 mM $MgCl_2$, 0.023 μkat glucose-6-phosphate dehydrogenase, 10 mM glucose and 0.047 μkat hexokinase (E.C.2.7.1.1). After an equilibration period of 6–8 min, the reaction was started by the sequential addition of glucose and hexokinase. The ATP content was calculated from the net increases in absorbance at 340 nm after the addition of glucose-6-phosphate dehydrogenase and hexokinase, respectively. The reaction medium for the assay of ADP contained 150 mM Tris-HCl, pH 8.1, 7.5 mM $MgCl_2$, 0.08 mM NADH, 2 mM PEP, 0.046 μkat lactate dehydrogenase (E.C. 1.1.1.27) and 0.067 μkat pyruvate kinase (E.C.2.7.1.40). After equilibration for 2–3 min, the reaction was started by the sequential addition of lactate dehydrogenase and pyruvate kinase. The content of ADP was calculated from the net decrease in absorbance at 340 nm after the addition of pyruvate kinase.

SUPPLEMENTARY DATA

Supplementary Data are available at *Molecular Plant Online*.

FUNDING

Financial support from the Deutsche Forschungsgemeinschaft (EM 166/1), and the Alexander-von-Humboldt (AvH) fellowship given to K.P. are gratefully acknowledged. While the major part of the work done by K.P. was supported by the AvH fellowship at the University of Osnabrueck, Germany, a minor part of the work was supported by a grant from the Department of Biotechnology (BT/PR 10272/GBD/27/85/2007), New Delhi, India. Initial contacts between the Hyderabad and the Osnabrueck group were facilitated by the DAAD/DST support (Project Nr D/02/32047).

ACKNOWLEDGMENTS

We thank Prof. H. Bauwe (Rostock) for probes and antiserum against GDC (P-protein). The authors thank Dr G.T. Hanke for critical reading of the manuscript, and H. Schwiderski for helping with its preparation. J. Backhausen, H. Metfies, J. Schlüter, A-L. Schön, and S. Heuer (Osnabrueck) helped with some of the experiments. H. Wolf-Wibbelmann cultivated the plants. No conflict of interest declared.

REFERENCES

Ahn, J.H. (2002). Noncompetitive RT–PCR. In A Laboratory Manual, Weigel D. and Glazebrook J., eds (Cold Spring Harbor, New York: Cold Spring Harbor Laboratory Press), pp. 174–176.

Amirsadeghi, S., Robson, C.A., McDonald, A.E., and Vanlerberghe, G.C. (2006). Changes in plant mitochondrial electron transport alter cellular levels of reactive oxygen species and susceptibility to cell death signaling molecules. Plant Cell Physiol. **47,** 1509–1519.

Atkin, O.K., Millar, A.H., Gardeström, P., and Day, D.A. (2000). Photosynthesis, carbohydrate metabolism and respiration in leaves of higher plants. In Photosynthesis: Physiology and Metabolism, Leegood R.C., Sharkey T.D., and von Caemmerer S., eds (London, The Netherlands: Kluwer Academic Publishers), pp. 153–175.

Bartoli, C.G., Gomez, F., Gergoff, G., Guiamét, J.J., and Puntarulo, S. (2005). Up-regulation of the mitochondrial alternative oxidase pathway enhances photosynthetic electron transport under drought conditions. J. Exp. Bot. **56,** 1269–1276.

Borecky, J., Nogueira, F.T., de Oliveira, K.A., Maia, I.G., Vercesi, A.E., and Arruda, P. (2006). The plant energy-dissipating mitochondrial systems: depicting the genomic structure and the expression profiles of the gene families of uncoupling protein and alternative oxidase in monocots and dicots. J. Exp. Bot. **57,** 849–864.

Bradford, M.M. (1976). A rapid and sensitive method for the quantitation of microgram quantities of protein utilizing the principle of protein–dye binding. Anal. Biochem. **72,** 248–254.

Carrari, F., Nunes-Nesi, A., Gibon, Y., Lytovchenko, A., Loureiro, M.E., and Fernie, A.R. (2003). Reduced expression of aconitase results in an enhanced rate of photosynthesis and marked shifts in carbon partitioning in illuminated leaves of wild species tomato. Plant Physiol. **133,** 1322–1335.

Clifton, R., Lister, R., Parker, K.L., Sappl, P.G., Elhafez, D., Millar, A.H., Day, D.A., and Whelan, J. (2005). Stress-induced co-expression of alternative respiratory chain components in *Arabidopsis thaliana*. Plant Mol. Biol. **58,** 193–212.

Clifton, R., Millar, A.H., and Whelan, J. (2006). Alternative oxidases in *Arabidopsis*: a comparative analysis of differential expression in the gene family provides new insights into function of non-phosphorylating bypasses. Biochim. Biophys. Acta. **1757,** 730–741.

Considine, M.J., Holtzapffel, R.C., Day, D.A., Whelan, J., and Millar, A.H. (2002). Molecular distinction between alternative oxidase from monocots and dicots. Plant Physiol. **129,** 949–953.

Day, D.A., and Wiskich, J.T. (1995). Regulation of alternative oxidase activity in higher plants. J. Bioenerg. Biomem. **27,** 379–385.

Dutilleul, C., Driscoll, S., Cornic, G., De Paepe, R., Foyer, C.H., and Noctor, G. (2003). Functional mitochondrial complex I is required by tobacco leaves for optimal photosynthetic performance in photorespiratory conditions and during transients. Plant Physiol. **131,** 264–275.

Elthon, T.E., Nickels, R.L., and McIntosh, L. (1989). Monoclonal antibodies to the alternative oxidase of higher plant mitochondria. Plant Physiol. **89,** 1311–1317.

Escobar, M.A., Geisler, D.A., and Rasmusson, A.G. (2006). Reorganization of the alternative pathways of the *Arabidopsis* respiratory chain by nitrogen supply: opposing effects of ammonium and nitrate. Plant J. **45,** 775–788.

Finnegan, P.M., Soole, K.L., and Umbach, A.L. (2004). Alternative mitochondrial electron transport proteins in higher plants. In Plant Mitochondria: From Genome to Function, Vol. 17, Advances in Photosynthesis and Respiration, Day D.A., Millar A.H., and Whelan J., eds (Dordrecht, The Netherlands: Kluwer Academic Press), pp. 163–230.

Fiorani, F., Umbach, A.L., and Siedow, J.N. (2005). The alternative oxidase of plant mitochondria is involved in the acclimation of shoot growth at low temperature: a study of *Arabidopsis* AOX1a transgenic plants. Plant Physiol. **139,** 1795–1805.

Gardeström, P., Igamberdiev, A.U., and Raghavendra, A.S. (2002). Mitochondrial functions in light. In Photosynthetic Nitrogen Assimilation and Associated Carbon and Respiratory Metabolism, Foyer C.H., and Noctor G., eds (The Netherlands: Kluwer Academic Publishers), pp. 151–172.

Gelhaye, E., et al. (2004). A specific form of thioredoxin *h* occurs in plant mitochondria and regulates the alternative oxidase. Proc. Natl. Acad. Sci. U S A. **101,** 14545–14550.

Genty, B., Briantais, J.M., and Baker, N.R. (1989). The relationship between the quantum yield of photosynthetic electron transport and quenching of chlorophyll fluorescence. Biochim. Biophys. Acta. **990,** 87–92.

Giraud, E., et al. (2008). The absence of alternative oxidase1a in Arabidopsis results in acute sensitivity to combined light and drought stress. Plant Physiol. **147,** 595–610.

Graeve, K., von Schaewen, A., and Scheibe, R. (1994). Purification, characterization, and cDNA sequence of glucose-6-phosphate dehydrogenase from potato (*Solanum tuberosum* L.). Plant J. **5,** 353–361.

Graham, D. (1980). Effects of light on dark respiration. In The Biochemistry of Plants: A Comprehensive Treatise, Davies D.D., ed. (New York: Academic Press), pp. 525–579.

Gray, G.R., Maxwell, D.P., Villarimo, A.R., and McIntosh, L. (2004). Mitochondria/nuclear signaling of alternative oxidase gene expression occurs through distinct pathways involving organic acids and reactive oxygen species. Plant Cell Rep. **23,** 497–503.

Gutierres, S., Sabar, M., Lelandais, C., Chétrit, P., Diolez, P., Degand, H., Boutry, M., Vedel, F., de Kouchkovsky, Y., and De Paepe, R. (1997). Lack of mitochondrial and nuclear-encoded subunits of complex I and alteration of the respiratory chain in *Nicotiana sylvestris* mitochondrial deletion mutants. Proc. Natl. Acad. Sci. U S A. **94,** 3436–3441.

Ho, L.H.M., Giraud, E., Lister, R., Thirkettle-Watts, D., Low, J., Clifton, R., Howell, K.A., Carrie, C., Donald, T., and Whelan, J. (2007). Characterization of the regulatory and expression

context of an alternative oxidase gene provides insights into cyanide-insensitive respiration during growth and development. Plant Physiol. **143,** 1519–1533.

Hoefnagel, M.H.N., Atkin, O.K., and Wiskish, J.T. (1998). Interdependence between chloroplasts and mitochondria in the light and the dark. Biochim. Biophys. Acta. **1366,** 235–255.

Igamberdiev, A.U., Shen, T., and Gardeström, P. (2006). Function of mitochondria during the transition of barley protoplasts from low light to high light. Planta. **224,** 196–204.

Juszczuk, I.M., and Rychter, A.M. (2003). Alternative oxidase in higher plants. Acta Biochem. Polonica. **50,** 1257–1271.

Krömer, S. (1995). Respiration during photosynthesis. Annu. Rev. Plant Physiol. Plant Mol. Biol. **46,** 45–70.

Krömer, S., and Scheibe, R. (1996). Function of the chloroplastic malate valve for respiration during photosynthesis. Biochem. Soc. Trans. **24,** 761–766.

Krömer, S., Malmberg, G., and Gardeström, P. (1993). Mitochondrial contribution to photosynthetic metabolism. A study with barley (*Hordeum vulgare*) leaf protoplasts at different light intensities and CO_2 concentrations. Plant Physiol. **102,** 947–955.

Lisec, J., Schauer, N., Kopka, J., Willmitzer, L., and Fernie, A.R. (2006). Gas chromatography mass spectrometry-based metabolite profiling in plants. Nature Protocols. **1,** 387–396.

Matsuo, M., and Obokata, J. (2006). Remote control of photosynthetic genes by the mitochondrial respiratory chain. Plant J. **47,** 873–882.

Maxwell, D.P., Wang, Y., and McIntosh, L. (1999). The alternative oxidase lowers mitochondrial reactive oxygen production in plant cells. Proc. Natl. Acad. Sci. U S A. **96,** 8271–8276.

Meeuse, B.J.D. (1975). Thermogenic respiration in aroids. Ann. Rev. Plant Physiol. Plant Mol. Biol. **26,** 117–126.

Millenaar, A.H., and Lambers, H. (2003). The alternative oxidase: *in vivo* regulation and function. Plant Biol. **5,** 2–15.

Noctor, G., De Paepe, R., and Foyer, C.H. (2007). Mitochondrial redox biology and homeostasis in plants. Trends Plant Sci. **12,** 125–134.

Noctor, G., Dutilleul, C., De Paepe, R., and Foyer, C.H. (2004). Use of mitochondrial electron transport mutants to evaluate the effects of redox state on photosynthesis, stress tolerance and the integration of carbon/nitrogen metabolism. J. Exp. Bot. **55,** 49–57.

Noguchi, K., and Yoshida, K. (2008). Interaction between photosynthesis and respiration in illuminated leaves. Mitochondrion. **8,** 87–99.

Nunes-Nesi, A., Carrari, F., Gibon, Y., Sulpice, R., Lytovchenko, A., Fisahn, J., Graham, J., Ratcliffe, R.G., Sweetlove, L.J., and Fernie, A.R. (2007a). Deficiency of mitochondrial fumarase activity in tomato plants impairs photosynthesis via an effect on stomatal function. Plant J. **50,** 1093–1106.

Nunes-Nesi, A., Carrari, F., Lytovchenko, A., Smith, A.M.O., Loureiro, M.E., Ratcliffe, R.G., Sweetlove, L.J., and Fernie, A.R. (2005). Enhanced photosynthetic performance and growth as a consequence of decreasing mitochondrial malate dehydrogenase activity in transgenic tomato plants. Plant Physiol. **137,** 611–622.

Nunes-Nesi, A., Sulpice, R., Gibon, Y., and Fernie, A.R. (2008). The enigmatic contribution of mitochondrial function in photosynthesis. J. Exp. Bot. **59,** 1675–1684.

Nunes-Nesi, A., Sweetlove, L.J., and Fernie, A.R. (2007b). Operation and function of the tricarboxylic acid cycle in the illuminated leaf. Physiol. Plant. **129,** 45–56.

Oliver, S.N., Lunn, J.E., Urbanczyk-Wochniak, E., Lytovchenko, A., Faix, B., van Dongen, J.T., Fernie, A.R., and Geigenberger, P. (2007b). Decreased expression of cytosolic pyruvate kinase in potato tubers leads to a decline in the level of pyruvate resulting in an *in vivo* repression of the alternative oxidase. Plant Physiol. **148,** 1640–1654.

Padmasree, K., and Raghavendra, A.S. (1999a). Importance of oxidative electron transport over oxidative phosphorylation in optimizing photosynthesis in mesophyll protoplasts of pea (*Pisum sativum* L). Physiol. Plant. **105,** 546–553.

Padmasree, K., and Raghavendra, A.S. (1999b). Prolongation of photosynthetic induction as a consequence of interference with mitochondrial oxidative metabolism in mesophyll protoplasts of pea (*Pisum sativum* L.). Plant Sci. **142,** 29–36.

Padmasree, K., and Raghavendra, A.S. (1999c). Response of photosynthetic carbon assimilation in mesophyll protoplasts to restriction on mitochondrial oxidative metabolism: Metabolites related to redox status and sucrose biosynthesis. Photosynth. Res. **62,** 231–239.

Padmasree, K., and Raghavendra, A.S. (2001). Consequence of restricted mitochondrial oxidative metabolism on photosynthetic carbon assimilation in mesophyll protoplasts: decrease in light activation of four chloroplastic enzymes. Physiol. Plant. **112,** 582–588.

Padmasree, K., Padmavathi, L., and Raghavendra, A.S. (2002). Essentiality of mitochondrial oxidative metabolism for photosynthesis: optimization of carbon assimilation and protection against photoinbition. Crit. Rev. Biochem. Mol. Biol. **37,** 71–119.

Pastore, D., Trono, D., Laus, M.N., Di Fonzo, N., and Flagella, Z. (2007). Possible plant mitochondria involvement in cell adaptation to drought stress: a case study: durum wheat mitochondria. J. Exp. Bot. **58,** 195–210.

Plaxton, W.C., and Podestá, F.E. (2006). The functional organization and control of plant respiration. Crit. Rev. Plant Sci. **25,** 159–198.

Priault, P., Fresneau, C., Noctor, G., De Paepe, R., Cornic, G., and Streb, P. (2006). The mitochondrial CMSII mutation of *Nicotiana sylvestris* impairs adjustment of photosynthetic carbon assimilation to higher growth irradiance. J. Exp. Bot. **57,** 2075–2085.

Raghavendra, A.S., and Padmasree, K. (2003). Beneficial interactions of mitochondrial metabolism with photosynthetic carbon assimilation. Trends Plant. Sci. **8,** 546–553.

Rasmusson, A.G., and Escobar, M.A. (2007). Light and diurnal regulation of plant respiratory gene expression. Physiol. Plant. **129,** 57–67.

Riazunnisa, K., Padmavathi, L., Scheibe, R., and Raghavendra, A.S. (2007). Preparation of *Arabidopsis* mesophyll protoplasts with high rates of photosynthesis. Physiol. Plant. **129,** 679–686.

Roessner-Tunali, U., Hegemann, B., Lytovchenko, A., Carrari, F., Bruedigam, C., Granot, D., and Fernie, A.R. (2003). Metabolic profiling of transgenic tomato plants overexpressing hexokinase reveals that the influence of hexose phosphorylation diminishes during fruit development. Plant Physiol. **133,** 84–99.

Rolleston, F.S. (1972). A theoretical background to the use of measured intermediates in the study of the control of intermediary metabolism. Curr. Top. Cell. Regul. **5,** 47–75.

Sabar, M., De Paepe, R., and de Kouchkovsky, Y. (2000). Complex I impairment, respiratory compensations, and photosynthetic decrease in nuclear and mitochondrial male sterile mutants of *Nicotiana sylvestris*. Plant Physiol. **124,** 1239–1249.

Saisho, D., Nakazono, M., Tsutsumi, N., and Hirai, A. (2001). ATP synthesis inhibitors as well as respiratory inhibitors increase steady-state level of alternative oxidase mRNA in *Arabidopsis thaliana*. J. Plant Physiol. **158,** 241–245.

Saradadevi, K., and Raghavendra, A.S. (1992). Dark respiration protects photosynthesis against photoinhibition in mesophyll protoplasts of pea *(Pisum sativum)*. Plant Physiol. **99,** 1232–1237.

Scheibe, R. (2004). Malate valves to balance cellular energy balance. Physiol. Plant. **120,** 21–26.

Scheibe, R., Backhausen, J.E., Emmerlich, V., and Holtgrefe, S. (2005). Strategies to maintain redox homeostasis during photosynthesis under changing conditions. J. Exp. Bot. **56,** 1481–1489.

Schreiber, U., Schliwa, U., and Bilger, W. (1986). Continuous recording of photochemical and non-photochemical chlorophyll fluorescence quenching with a new type of modulation fluorometer. Photosynth. Res. **10,** 51–62.

Shyam, R., Raghavendra, A.S., and Sane, P.V. (1993). Role of dark respiration in photoinhibition of photosynthesis and its reactivation in the cyanobacterium *Anacystis nidulans*. Physiol. Plant. **88,** 446–452.

Siedow, J.N., and Umbach, A.L. (2000). The mitochondrial cyanide–resistant oxidase: structural conservation amid regulatory diversity. Biochem. Biophys. Acta. **1459,** 432–449.

Sieger, S.M., Kristensen, B.K., Robson, C.A., Amirsadeghi, S., Eng, E.W., Abdel-Mesih, A., Møller, I.M., and Vanlerberghe, G.C. (2005). The role of alternative oxidase in modulating carbon use efficiency and growth during macronutrient stress in tobacco cells. J. Exp. Bot. **56,** 1499–1515.

Singh, K.K., Shyam, R., and Sane, P.V. (1996). Reactivation of photosynthesis in the photoinhibited green alga *Chlamydomonas reinhardtii*: Role of dark respiration and light. Photosynth. Res. **49,** 11–20.

Sweetlove, L.J., Lytovchenko, A., Morgan, M., Nunes-Nesi, A., Taylor, N.L., Baxter, C.J., Eickmeier, I., and Fernie, A.R. (2006). Mitochondrial uncoupling protein is required for efficient photosynthesis. Proc. Natl Acad. Sci. U S A. **103,** 19587–19592.

Tcherkez, G., Cornic, G., Bligny, R., Gout, E., and Ghashghaie, J. (2005). *In vivo* respiratory metabolism of illuminated leaves. Plant Physiol. **138,** 1596–1606.

Umbach, A.L., Fiorani, F., and Siedow, J.N. (2005). Characterization of transformed *Arabidopsis* with altered alternative oxidase levels and analysis of effects on reactive oxygen species in tissue. Plant Physiol. **139,** 1806–1820.

Vanlerberghe, G.C., and McIntosh, L. (1997). Alternative oxidase: from gene to function. Annu. Rev. Plant Physiol. Plant Mol. Biol. **48,** 703–734.

Vanlerberghe, G.C., and Ordog, S.H. (2002). Alternative oxidase: Integrating carbon metabolism and electron transport in plant respiration. In Photosynthetic Nitrogen Assimilation and Associated Carbon and Respiratory Metabolism, Foyer C.H., and Noctor G., eds (The Netherlands: Kluwer Academic Publishers), pp. 173–191.

Voss, I., Koelmann, M., Wojtera, J., Holtgrefe, S., Kitzmann, C., Backhausen, J.E., and Scheibe, R. (2008). Knockout of major leaf ferredoxin reveals new redox–regulatory adaptations in *Arabidopsis thaliana*. Physiol. Plant. **133,** 584–598.

Yoshida, K., Terashima, I., and Noguchi, K. (2006). Distinct roles of the cytochrome pathway and alternative oxidase in leaf photosynthesis. Plant Cell Physiol. **47,** 22–31.

Yoshida, K., Terashima, I., and Noguchi, K. (2007). Up-regulation of mitochondrial alternative oxidase concomitant with chloroplast over-reduction by excess light. Plant Cell Physiol. **48,** 606–614.

Yoshida, K., Watanabe, C., Kato, Y., Sakamoto, W., and Noguchi, K. (2008). Influence of chloroplastic photo-oxidative stress on mitochondrial alternative oxidase capacity and respiratory properties: a case study with *Arabidopsis yellow variegated 2*. Plant Cell Physiol. **49,** 592–603.

Zarkovic, J., Anderson, S.L., and Rhoads, D.M. (2005). A reporter system used to study developmental expression of alternative oxidase and isolate mitochondrial retrograde regulation mutants in *Arabidopsis*. Plant Mol. Biol. **57,** 871–888.

Zsigmond, L., Rigó, G., Szarka, A., Székely, G., Ötvös, K., Darula, Z., Medzihradszky, K.F., Koncz, C., Koncz, Z., and Szabatos, L. (2008). *Arabidopsis* PPR40 connects abiotic stress responses to mitochondrial electron transport. Plant Physiol. **149,** 1721–1737.